

RESEARCH ARTICLE

Numerical Simulation of Thermal Comfort in Passenger Car Compartment Using CFD-Heat Transfer Coupling

Muhammad Afiq Mohd Reza, Wan Naimah Wan Ab Naim and Mohd Jamil Mohamed Mokhtarudin*

Faculty of Manufacturing and Mechatronic Engineering Technology, Universiti Malaysia Pahang Al-Sultan Abdullah, 26600 Pekan, Pahang, Malaysia

ABSTRACT - While heating, ventilation, and air conditioning (HVAC) systems provide thermal comfort for the car occupants, the passenger compartment's thermal environment is not uniform and needs to be further assessed. Different cars have different car compartment designs too, thus, the distribution of the airflow and temperature field inside the passenger compartment has to be examined so that improvements in the different car designs can be proposed. Hence, this study aims to investigate the thermal comfort in a Malaysian local brand sedan car which is Proton Saga FLX 2012 using the coupling of computational fluid dynamics (CFD) and heat transfer. A simplified human model was included in the car to allow the understanding of the effect of airflow and temperature field distribution on the passengers sitting under ventilation system conditions. A few conditions also were simulated; without outlets where all windows close (Case 1) and with different window openings (Case 2). The thermal comfort of the passengers was analysed based on the temperature or thermal field displayed on the human models. The head, hand, torso, feet and overall temperature were evaluated. The results showed that in the no outlet condition when all windows were closed, air conditions were on and the initial compartment temperature was at 50°C, it can cause hyperthermia stage to humans. Besides, the hands will have the lowest body temperature in both situations with and without window openings because it is directly facing the air-conditioning. In addition, window opens have pleasant air velocity compared to those without windows open.

ARTICLE HISTORY

Received : 14th Jan 2024
Revised : 15th March 2024
Accepted : 30th April 2024
Published : 5th May 2024

KEYWORDS

Thermal Comfort
Hyperthermia
HVAC
CFD
Bio-heat transfer

1.0 INTRODUCTION

The human body maintains its internal temperature through homeostasis. The hypothalamus regulates body temperature by determining a 'set point,' or the temperature at which it should be maintained, which is around 37°C [1, 2]. Maintaining the whole human body's heat balance and also the local heat balance of parts of the human body such as the head, arms, and feet is also known as thermal comfort [1]. Thermal discomfort could lead to heat illness [3, 4].

Heat illness is best thought of as a sequence of disorders that proceed from heat fatigue to heat injury and heat stroke along a continuum of increasing severity [5]. Heat fatigue is a mild to moderate type of heat illness marked by an inability to maintain cardiac activity, as well as a moderate to extreme increase in body temperature, nausea, and dry skin due to a lack of sweating or anhidrosis [6]. Meanwhile, heat injury is characterized by damage to the organ and tissue when the body temperature is elevated, which has more serious consequences than heat fatigue. It could lead to organ failure, which usually is undetectable and its symptoms are difficult to differentiate from heat fatigue [7]. On the other hand, heat stroke is described as a significant increase in body temperature and it can become lethal when the core body temperature rises more than 40°C, which is called a hyperthermia state [5, 8]. Due to poor heat dissipation, this condition will trigger a critical systemic inflammatory response, that will cause a multi-organ failure [9].

Human body temperature is highly variable and can vary depending on several factors, i.e. the surrounding temperatures where the exposure to extreme heat than average conditions compromises the body's ability to regulate temperature and can result in a heat illness [10]. Thus, understanding how the human body reacts to temperature changes can be beneficial especially in Malaysia, where each year the climate is mostly hot and humid. With the hot weather and as most Malaysians are using cars as a main transportation, the study on human body temperature reaction inside a car will give useful information, particularly in determining the causes of discomfort in a car compartment. Thermal discomfort in the passenger compartment could lead to death, for example, if sitting in a parked vehicle on hot days, which may result in heat stroke or hyperthermia [11]. Numerous cases of hyperthermia death especially in children due to sitting in parked vehicles were reported in the United States, Europe, and recently in Malaysia [12].

The thermal environment in cars depends on the interior volume, complexity of the interior structure, position of the passenger, and microclimate conditions [13, 14]. The common layout of the passenger compartments in most cars consists of the dashboard that has a vent for air flowing inside the compartment, the front, door and rear window that allow for

thermal radiation exposure, and the front and rear seats. From this, a car compartment resembles a greenhouse which has little to no ventilation hence it can generate the greenhouse effect which on hot days, the temperature can rise up to 70°C [15]. Thus, the interior part of the car needs to be designed so as to provide optimum comfort.

To provide comfort, heating, ventilation, and air conditioning (HVAC) systems were employed in cars, whose primary function is to provide quality indoor air flow and thermal comfort for the occupants. The car occupants can control the temperature and environment in the car to suit their needs. While HVAC systems have the capability of giving sufficient cooling and heat, the passenger compartment thermal environment is not uniform and the thermal effects need to be assessed and examined in a measurable expression [1]. In addition, different cars have different car compartment designs too. Therefore, it is necessary to investigate the distribution of the airflow and temperature field inside the passenger compartment so that improvements in the car design can be proposed.

Hence, this study aims to investigate the thermal comfort in a Malaysian local brand sedan car which is Proton Saga FLX 2012 using the coupling of computational fluid dynamics (CFD) and heat transfer. A simplified human model was included in the car model to allow the understanding of the effect of airflow and temperature field distribution in the car on the passengers sitting under ventilation system conditions. A few conditions also were simulated; without outlets where all windows close (Case 1) and with different window openings (Case 2). Lastly, the passenger comfort was analysed.

2.0 METHODS

A detailed description of the methodology will be discussed below.

2.1 Passenger Compartment Geometry Model

A car model geometry based on the Proton Saga FLX 2012 was developed using Solidworks 2020. The car exterior geometry (shown in Figure 1 (a)) was developed by using the parameters taken from the actual dimensions of the car (values shown in Table 1). The car exterior and interior parts with human geometry are shown in Figure 1. Then, the geometries were assembled in COMSOL Multiphysics 5.4 (COMSOL AB, Sweden) as shown in Figure 2. It consists of five seats which is a typical configuration of a sedan car (Figure 1 (b)). However, the center console which is the part where the cup holders and the hand brake were placed, was not developed since it will not have any significant effect on the results. The dashboard of the car consists of four air conditioning vents, a steering wheel and a meter cluster (Figure 1 (c)). In this project, there were two human models will be placed in front seats. The hands of the human models (both the driver and the passenger) will be raised to simulate the situation during the driving condition (Figure 1 (d)).

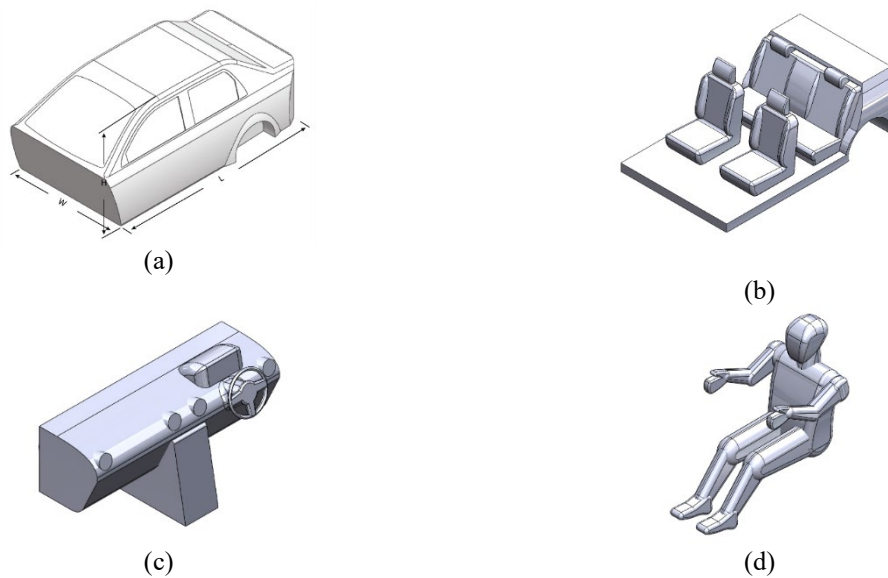


Figure 1. Geometry of car exterior and interior parts with human geometry. (a) The car exterior geometry where L=length, W=width and H=height; (b) Five seats, a configuration of a sedan car; (c) the dashboard of the car; (d) the human geometry

Table 1. Dimensions used to develop the car exterior geometry

Parameters	Values
L	3115 mm
W	1700 mm
H	1920 mm

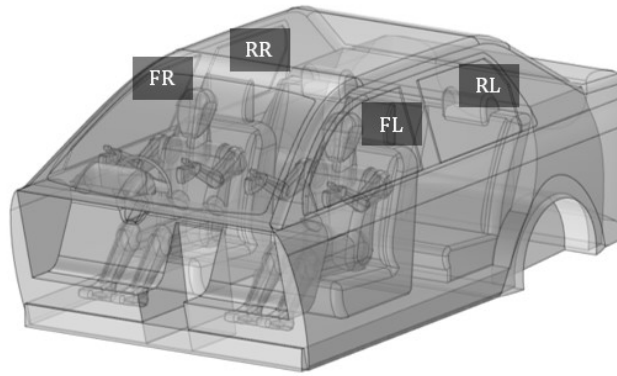


Figure 2. A complete car geometry model based on the Malaysian local brand sedan Proton Saga FLX 2012. FR= Front right, FL= Front left, RL= Rear Left, and RR= Rear Right

2.2 Governing Equations

The simulation involves the fluid flow equation, heat transfer equation, and the bio-heat equation based on Penne's approximation to solve the bio-heat transfer between the human and the environment. Details are described below.

2.2.1 Fluid Flow of Air

In this work, the turbulent model was used for the air-fluid flow. The turbulent flow was solved using the Reynolds-averaged Navier-Stokes (RANS) equations. Because of its high performance for indoor airflows and low computing cost [16], the k - ϵ turbulence model with realizability constraints was chosen to simulate the turbulence effects as shown in Equations 1 and 2. Wall functions were used to represent flow near walls.

$$\rho(u \cdot \nabla)k = \nabla \cdot \left[\left(\mu + \frac{\mu_T}{\sigma_k} \right) \nabla k \right] + P_k - \rho \epsilon \quad (1)$$

$$\rho(u \cdot \nabla)\epsilon = \nabla \cdot \left[\left(\mu + \frac{\mu_T}{\sigma_\epsilon} \right) \nabla \epsilon \right] + C_{\epsilon 1} \frac{\epsilon}{k} P_k - C_{\epsilon 2} \rho \frac{\epsilon^2}{k} \quad (2)$$

Here, ρ = density, u = velocity, k = turbulent kinetic energy, μ = dynamic viscosity, μ_T = turbulent viscosity, ϵ = turbulent dissipation rate, $\sigma_k = 1.0$, $\sigma_\epsilon = 1.3$, $C_{\epsilon 1} = 1.44$ and $C_{\epsilon 2} = 1.92$, respectively. Material properties for thermal comfort calculation were shown in Table 2 [17, 18].

2.2.2 Heat Transfer

The air temperature and the seats were modeled using the heat transfer model that can be described using the following Equation 3:

$$\rho C_p u \cdot \nabla T + \nabla \cdot q = Q \quad (3)$$

Here, ρ = density, C_p = heat capacity at constant pressure, u = velocity field, $q = (-k \nabla T)$, k = thermal conductivity and Q = heat source. Material properties for thermal comfort calculation were shown in **Table 2** [17, 18].

2.2.3 Bio-heat Transfer Model

Heat transfer throughout biological tissue was modeled using the bio-heat equation based on Penne's approximation. The equation was similar to the conventional heat transfer equation as shown in Equation 3, but the rate of heat transfer from blood to tissue and the rate of metabolic heat production in the tissue were included as shown in Equation 4 [17].

$$\rho C_p u \cdot \nabla T + \nabla \cdot q = Q + Q_{bio} \quad (4)$$

Here, ρ = density, C_p = heat capacity at constant pressure, u = velocity field, $q = (-k \nabla T)$, k = thermal conductivity, Q = heat source and $Q_{bio} = \rho_b C_{p,b} \omega_b (T_b - T) + Q_{met}$. Q_{met} = metabolic heat source. Material properties for thermal comfort calculation were shown in **Table 2** [17, 18].

Table 2. Material properties for thermal comfort calculation

Material	Human Skin	Seat Polyurethane foam	Dashboard ABS plastic	Window Glass
Heat capacity at constant pressure, C_p [J/(kg * K)]	3589	1685.60	1480.6	754
Density, ρ [kg/m ³]	1200	70	996.3	2529.5
Thermal conductivity, k [W/(m * K)]	0.24	0.05	2.7	1.171

2.3 Boundary and Initial Conditions

For the bio-heat transfer model, only the skin boundary condition was applied, as stated in Equation 5.

$$-k \frac{\partial T}{\partial x} = h(T - T_a) + \sigma \epsilon [(T + 273)^4 - (T_a + 273)^4] + (3.054 + 16.7hw_{skin})(0.256T - 3.37 - P_a) \tag{5}$$

Here, h , T , and T_a were heat transfer coefficient, tissue temperature and ambient temperature, respectively. σ , ϵ , w_{skin} and P_a were Stefan-Boltzmann constant, emissivity, skin wittedness and water vapour pressure in the air, respectively.

Since this work simulates different conditions of ventilation inside the car compartments. i.e. a case where the car has no outlets (all windows close) (Case 1) and with different window openings (Case 2), different boundaries and initial condition were imposed (Tables 3 and 4). For Case 1 where all the windows closed, the car compartment was set to have no outlet. The airflow will recirculate inside the compartment. Meanwhile, the inlet airflow was set to have two setups or conditions which are (1) with air conditioning (WAC) and (2) without air conditioning (WOAC). The initial temperature of the compartment will have a variation of 10°C, 30°C and 50°C for both conditions. For the WAC condition, the mass flow rate at the inlet of the dashboard was set to be 0.03247 kg/s with a temperature of 10°C for the airflow entering the car compartment. Airflow was configured to recirculate inside the compartment itself. On the other hand, for the WOAC condition, the mass flow rate at the inlet of the dashboard was set to be 0 kg/s (to represent the condition without air conditioning) with a temperature of 10°C for the airflow entering the car compartment. Detailed boundary and initial conditions for Case 1 are shown in Table 3. The result of the simulation for these conditions will be based on the initial temperature of the compartment which was 10°C, 30°C and 50°C.

On the other hand, for Case 2, five different ventilation systems or window openings were set which were front left (FL), front left and rear left (FL-RL), front left and right (FL-FR), rear left (RL) and rear left and right (RL-RR) windows. The location of each window was labelled as shown in Figure 2. For this case the inlet airflow was set to 0.03247 kg/s of mass flow rate, meaning it has air conditioning and the temperature was set to 10°C inlet air temperature. The initial compartment temperature was set to 30°C. The outlet where the window opens had a constant atmospheric pressure. Detailed boundary and initial conditions for Case 2 are shown in Table 4. The windshield, seats, side and rear windows, and the interior floor were all subjected to no-slip wall boundary conditions. The interior surfaces had an emissivity of 0.95, whereas the glass had an emissivity of 0.88 [16].

2.4 Numerical Implementation

The geometries were meshed with tetrahedral elements. The meshing element for tetrahedral mesh was 410559 elements which was set for both fluid and solid models. The fluid flow equation together with the heat transfer model and the bio-heat equation based on Penne’s approximation were solved concurrently using the standard direct solver included in the COMSOL Multiphysics 5.4 (COMSOL AB, Sweden).

Table 3. Boundary and initial conditions for Case 1

Case 1	Inlet		Outlet	Compartment Temperature
	Mass flow rate	Initial temperature		
With air condition (WAC)	0.03247 kg/s	10°C	0 kPa	10°C
		10°C	0 kPa	30°C
		10°C	0 kPa	50°C
Without air conditioning (WOAC)	0 kg/s	10°C	0 kPa	10°C
		10°C	0 kPa	30°C
		10°C	0 kPa	50°C

Table 4. Boundary and initial conditions for Case 2

Case 2 (window openings)	Inlet		Outlet				Compartment Temperature
	Mass flow rate	Initial temperature	FL	FR	RL	RR	
Front left (FL)	0.03247 kg/s	10°C	101.325 kPa	0 kPa	0 kPa	0 kPa	30°C
Front left and rear left (FL-RL)	0.03247 kg/s	10°C	101.325 kPa	0 kPa	101.325 kPa	0 kPa	30°C
Front left and right (FL-FR)	0.03247 kg/s	10°C	101.325 kPa	101.325 kPa	0 kPa	0 kPa	30°C
Rear left (RL)	0.03247 kg/s	10°C	0 kPa	0 kPa	101.325 kPa	0 kPa	30°C

Rear left and right (RL-RR)	0.03247 kg/s	10°C	0 kPa	0 kPa	101.325 kPa	101.325 kPa	30°C
-----------------------------	--------------	------	-------	-------	-------------	-------------	------

3.0 RESULTS

Since this work simulates different conditions of ventilation inside the car compartments, the results will be divided based on the case studied.

3.1 Case 1: No Outlet Condition

3.1.1 With Air Conditioning (WAC)

Figure 3 illustrates the airflow streamline and thermal field of the human models for the mentioned condition. The overall average surface temperature of the human models for initial compartment temperatures of 10°C, 30°C and 50°C were 21.33°C, 33.69°C and 46.05°C, respectively. For initial compartment temperatures of 10°C, the torso has the lowest temperature and for 30°C and 50°C, it is more uniform across the entire body and colder temperatures at the head, hands and feet, respectively.

Based on corresponding temperature conditions for human body parts [16], the permissible vertical temperature differential between the head and feet for the human body should be less than 3°C. Table 5 represents the local temperature of head, hand, torso and feet of the human models. The temperature between each body part only has around 1°C to 2°C temperature differences for all initial compartment temperature which was felt within the range of acceptable conditions [16].

The airflow streamlines have an interesting pattern as it travels from the dashboard vents to the rear seat and the recirculation zone was observed in the rear seat region recirculates again at the human sitting position at the front seats. Lower initial compartment temperature produced more streamlines and as the temperature gets higher, streamlines become lesser. The passenger's legs divert a portion of the air entering the front compartment's legroom area from the back of a car, as well as airflow from the inlet or dashboard vents, towards the face region, which is regarded as unpleasant for passengers with breathing issues [16].

3.1.2 Without Air Conditioning (WOAC)

Figure 4 shows the result of the surface temperature of WOAC of no outlet conditions for three different compartment temperatures. The overall average surface temperature of the human models for initial temperatures of 10°C, 30°C and 50°C were 28.21°C, 29.88°C and 31.58°C, respectively. The thermal field was uniform throughout the human body. No signs of airflow were presented in the simulated result which was expected since the inlet airflow was set to 0 kg/s mass flow rate.

3.2 Case 2: With Different Window Openings

Table 5 and Figure 5 shows the simulated result of the described case. For FL and RL, it resulted in an average temperature of the human model of 29.55°C and 29.42°C, respectively. Furthermore, for FL-FR, FL-RL and RL-RR the average temperatures are 29.85°C, 29.31°C and 29.53°C, respectively.

Meanwhile, Figure 6 shows the result of the airflow streamlines with arrowheads to help indicate the flow of the air to the dedicated outlets or window openings that were circled in the figure. The air velocity around the driver and passenger across all ventilation systems achieved a similar pattern which is around 0.6 m/s. Due to the deflection of the air as the front seats obstruct the airflow from the inlet vents, a recirculation zone was observed in the rear seat region. The human's legs deflected a portion of the air entering the front compartment's legroom space from the rear seat, as well as airflow from inlet openings. All ventilation systems have the same local temperature at the human's feet of 29.85°C. This can be caused by the lack of air in the legroom space in the car compartment. Meanwhile, the hands showed the lowest temperature compared to other body portions. The hands of the human models were the closest to the inlet vents which resulted in that portion of the human model having a colder thermal field across all ventilation systems at a temperature of around 26°C.

The location at which window openings play a role in the thermal field and overall average temperature of the human models. To give an example, based on the result as explained above and also as presented in Table 5, Figure 5 and Figure 6, the FL-FR ventilation system has the highest average temperature compared to the rest which is 29.85°C. The reason is, since both front windows open, most of the cold air from the air conditioning of the car escapes through the front windows compared to the FL-RL and RL-RR, the cold air needed to pass through the human models before exiting through the windows. Also, opening the car window at one side such as FL and RL, achieves a colder average temperature of the human models compared to when both windows are open.

Most of the results of the average human models' temperature obtained in Table 6 also show a hypothermia stage (temperature below 35°C) except for Case 1/WAC at 50°C initial compartment temperature where it showed hyperthermia stage (temperature more than 40°C). The hypothermia stages for these results were mild, for temperatures around 35°C and 33°C, and moderate hypothermia, for temperatures around 32°C and 29°C [25]. Mild hypothermia can cause physical

changes such as maximal shivering, amnesia and ataxia. Moderate hyperthermia can cause a state of near-unconsciousness or insensibility

To compare using Table 6 between Case 1 and Case 2 which has air conditioning conditions with a 30°C compartment initial temperature, Case 2 has significantly lower average human models' temperature at all types of ventilation systems by around 4°C compared to Case 1. Other than that, comparing both Case 1/WAC and Case 1/WOAC conditions, the average human model temperature resulted in significantly lower temperature without air conditioning conditions for compartment initial temperature of 30°C and 50°C by around 4°C and 15°C lower, respectively. For compartment's initial temperature of 10°C, the Case 1/WAC temperature a lower temperature value around 7°C difference.

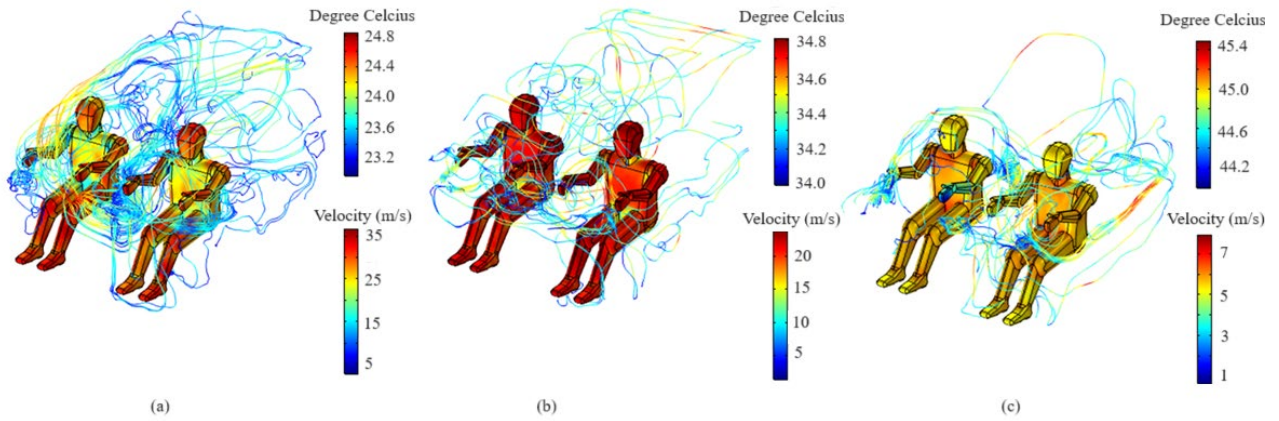


Figure 3. Case 1/WAC results. Initial compartment temperature: (a) 10°C, (b) 30°C and (c) 50°C

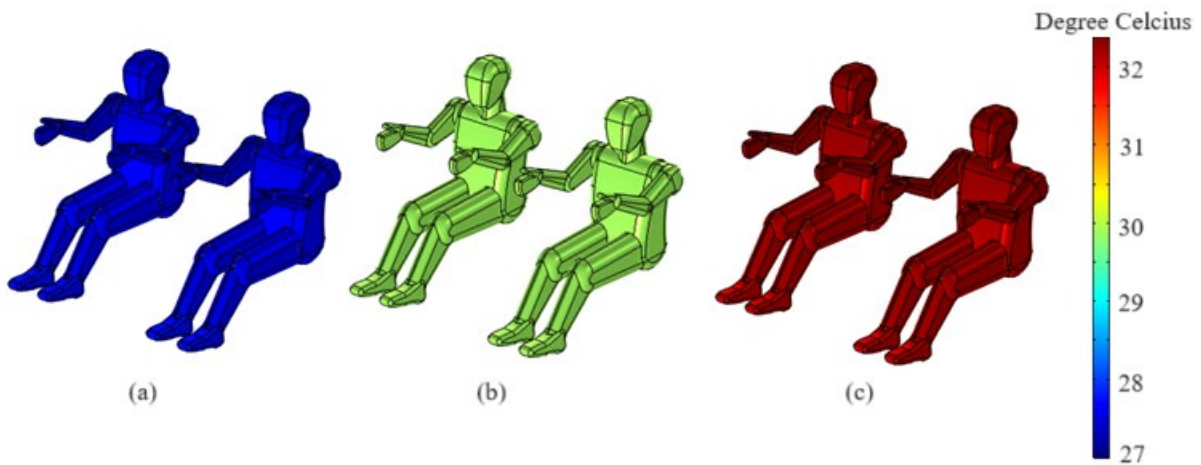


Figure 4. Case 1/WOAC. Initial compartment temperature: (a) 10°C, (b) 30°C and (c) 50°C

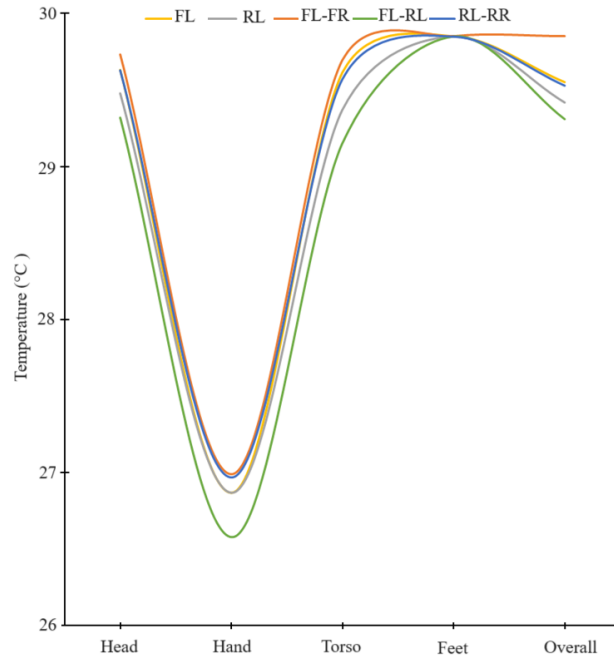


Figure 5. Local temperature of Case 2

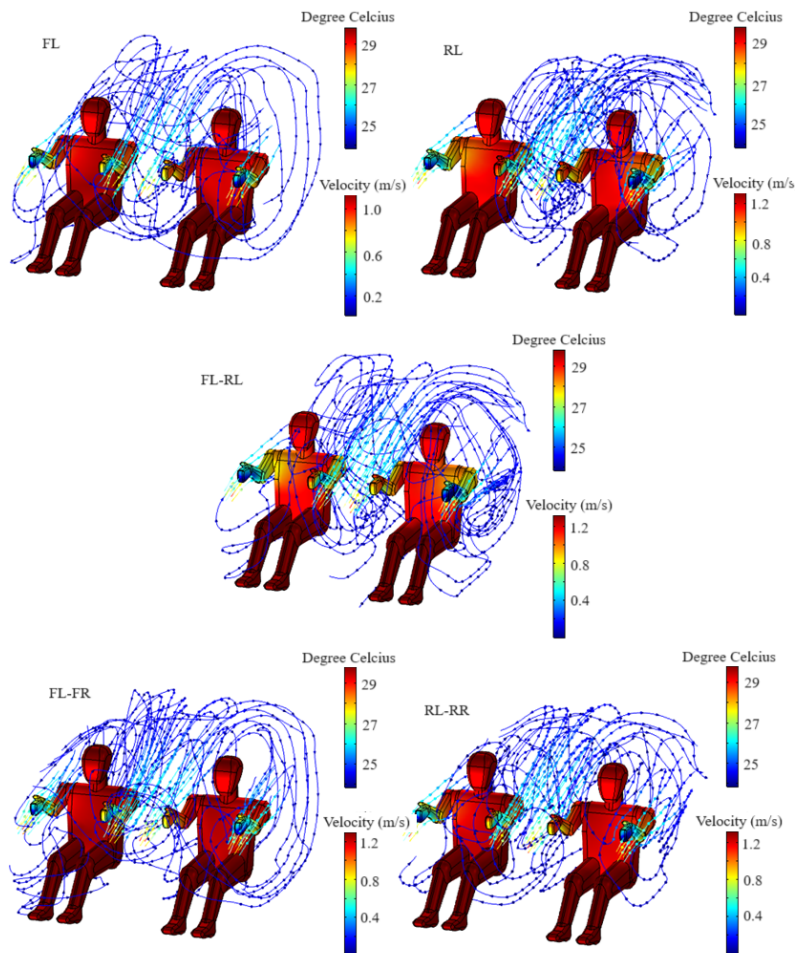


Figure 6. Case 2 results

Table 5. Local temperature of Cases 1 and 2

	Local Temperature (°C)				
	Head	Hand	Torso	Feet	Overall
Case 1					
Initial Temperature (°C)					
10	24.42	24.20	23.68	24.42	21.33
30	34.47	34.66	34.49	34.86	33.69
50	45.01	44.90	45.26	45.02	46.05
Case 2					
Ventilation systems					
FL	29.63	26.87	29.61	29.85	29.55
RL	29.48	26.87	29.37	29.85	29.42
FL-FR	29.73	26.99	29.69	29.85	29.85
FL-RL	29.32	26.58	29.15	29.85	29.31
RL-RR	29.63	26.97	29.57	29.85	29.53

Table 6. Overall average temperature for all cases and conditions

Case	Condition	Average Temperature (°C)
With air conditioning (WAC)		
No outlet (Case 1)	10°C	21.33
	30°C	33.69
	50°C	46.05
	Without air conditioning (WOAC)	
	10°C	28.21
	30°C	29.88
With window openings (Case 2)	50°C	31.58
	Ventilation system	
	FL	29.55
	RL	29.42
	FL-FR	29.85
	FL-RL	29.31
	RL-RR	29.53

4.0 DISCUSSION

Understanding the car's thermal environment is crucial to obtaining an adequate degree of thermal comfort. Two cases which were no outlet (with and without air conditioning) and with different window openings were simulated to investigate how the human models would respond to it with the addition of various car compartment temperatures.

Based on Table 6, Case 1 (no outlet condition) /WAC at 50°C initial compartment temperature showed hyperthermia stage (temperature more than 40°C). Hyperthermia in passenger compartments is more common among children as they lack thermoregulation efficiency compared to adults [9]. This hyperthermia situation might have contributed to the cause of the dead children when they were left in the car at high temperatures (usually at noon when the parents were working) for long hours. A mechanism should be made to avoid this situation in the future.

Besides that, based on Tables 4 and 5, in most of the situations/conditions in both Cases 1 and 2, the hands showed the lowest temperature compared to other body portions. The hands of the human models were the closest to the inlet vents which resulted in that portion of the human model having a colder thermal field. Cold thermal discomfort is frequently linked to localized thermal stress at human extremities (toes, fingers) or exposed surfaces (ears, nose). To prevent this, the inlet vents can be directed towards the head or torso more and also adding an inlet at the legroom space to stabilize the local temperature of the human models.

In addition, in comparison to Cases 1 and 2, Case 2 (values) air velocity appeared to have a lower value compared to Case 1 (values). The American Society of Heating, Refrigerating and Air-Conditioning Engineers (ASHRAE) standard recommends 1 m/s for pleasant air velocity [19]. Higher values can cause unpleasant cooling of sensitive body parts like the neck, eyes, and head. Case 2 air velocity appears to have a value that lies under the standard that ASHRAE recommends for pleasant air velocity which is under 1 m/s. While a larger value of air velocity was present in Case 1 which can affect the comfort level of the passengers. Moreover, the airflow of Case 2 shows a smoother streamline compared to Case 1.

In comparison with previous studies by Dixit et al. [17] and Khatoun et al. [16] who showed more variations in terms of the thermal field across the human models, the thermal distribution in this work was more uniform. Instead of steady state simulation like ours, they used transient conditions and Fanger's model to determine the thermal comfort satisfactory level of the human models.

However, comparable to Dixit et al. [17], this work used an actual car compartment model. No other previous studies used the car compartment which was based on the actual Malaysian local brand car Proton Saga. Furthermore, this project takes into account the different window openings as a ventilation system where the airflow streamlines in response to the human thermal field can be observed. Other than that, this project also considers a case of airflow recirculating inside the car compartment to best suit the real scenario.

4.1 Limitation and Future Work

This project does not include the standard scales usually used to represent thermal discomfort such as Fanger's thermal comfort assessment, PMV and PPD [16-18, 20], thus, in the future, details work including related standard scales should be made. Furthermore, the CAD model utilized was a fairly old car model. In the future, a newer car model can be considered to adapt to the latest design structure of the car compartment. A newer model for example is the Proton X70 and X50. Both models have excellent and premium interior design. This way, the thermal comfort which consists of airflow and heat transfer simulation can be studied according to the latest design engineering. Besides that, the current CFD and heat transfer simulation study was computed as a stationary study. This is due to the time constraints and restriction of the computer power that leads to the selected computation rather than the most preferable time-dependent study or transient computation. Time dependent studies can be implemented in the future.

Moreover, a better understanding of thermal comfort in a vehicle can also be investigated using particle image velocimetry (PIV), such as has been done in [21]. The numerical analysis performed can be validated using the PIV technique by measuring the thermal convection generated in the chamber. However, a suitable experimental setup is needed to perform the validation process using PIV [22].

5.0 CONCLUSION

The thermal comfort of the passengers was analyzed based on the temperature or thermal field displayed on the human models themselves. The head, hand, torso, feet and overall temperature were produced to evaluate which part was more affected by the set conditions. Based on that, it was examined whether the temperatures were able to result in thermally satisfied for the passengers. The results showed that in the no outlet condition when all windows are closed and air-conditions are on and the initial compartment temperature is at 50°C, it can cause hyperthermia stage to the human. Besides, the hands will have the lowest body temperature in both situations with and without window openings because it is directly facing the air-conditioning. In addition, window opens have pleasant air velocity compared to windows open.

6.0 CONFLICT OF INTEREST

The authors declare no conflicts of interest.

7.0 AUTHORS CONTRIBUTION

M. A. Mohd Reza (Methodology; Data curation; Formal analysis; Writing - original draft; Resources)

W. N. Wan Ab Naim (Writing - original draft; Writing - review & editing)

M. J. Mohamed Mokhtarudin (Writing - review & editing; Project administration; Supervision)

8.0 ACKNOWLEDGEMENTS

This study was not supported by any grants from funding bodies in the public, private, or not-for-profit sectors.

9.0 REFERENCES

- [1] Holmer I, Nilsson H, Bohm M, Noren O. Thermal aspects of vehicle comfort. *Applied Human Science*. 1995;14(4):159-65.
- [2] Satinoff E, Hendersen R. Thermoregulatory behavior. *Handbook of operant behavior*: Routledge; 2022. p. 153-73.
- [3] Luo M, Xu S, Tang Y, Yu H, Zhou X, Chen Z. Dynamic thermal responses and showering thermal comfort under different conditions. *Building Environment*. 2023;237:110322.
- [4] Ravindra K, Agarwal N, Mor S. Assessment of thermal comfort parameters in various car models and mitigation strategies for extreme heat-health risks in the tropical climate. *Journal of Environmental Management*. 2020;267:110655.
- [5] Leon LR, Bouchama A. Heat stroke. *Compr Physiol*. 2011;5(2):611-47.
- [6] Worfolk JB. Heat waves: their impact on the health of elders. *Geriatric Nursing*. 2000;21(2):70-7.
- [7] Leon LR, Helwig BG. Heat stroke: role of the systemic inflammatory response. *Journal of Applied Physiology*. 2010;109(6):1980-8.

- [8] Bouchama A, Abuyassin B, Lehe C, Laitano O, Jay O, O'Connor FG, et al. Classic and exertional heatstroke. *Nature Reviews Disease Primers*. 2022;8(1):8.
- [9] Booth JN, Davis GG, Waterbor J, McGwin G. Hyperthermia deaths among children in parked vehicles: an analysis of 231 fatalities in the United States, 1999–2007. *Forensic Science, Medicine, and Pathology*. 2010;6:99-105.
- [10] Yousef H, Ramezanpour Ahangar E, Varacallo M. Physiology, thermal regulation. *StatPearls*. 2022.
- [11] McLaren C, Null J, Quinn J. Heat stress from enclosed vehicles: moderate ambient temperatures cause significant temperature rise in enclosed vehicles. *Pediatrics*. 2005;116(1):e109-e12.
- [12] Ahad R, Rosli NS, Mustafa MZ. Child Presence Detection Car Alarm System using GSM. *Research Innovation in Technical Vocational Education Training*. 2021;1(2):028-41.
- [13] Simion M, Socaciu L, Unguresan P. Factors which influence the thermal comfort inside of vehicles. *Energy Procedia*. 2016;85:472-80.
- [14] Bandi P, Manelil NP, Maiya M, Tiwari S, Thangamani A, Tamalapakula J. Influence of flow and thermal characteristics on thermal comfort inside an automobile cabin under the effect of solar radiation. *Applied Thermal Engineering*. 2022;203:117946.
- [15] Siddiqui SA, Siddiqui GF, Singh MV. Vehicular hyperthermia deaths in Indian children: a little recognised mode of fatal injury. *Tropical doctor*. 2021;51(1):109-11.
- [16] Khatoon S, Kim M-H. Thermal comfort in the passenger compartment using a 3-D numerical analysis and comparison with Fanger's comfort models. *Energies*. 2020;13(3):690.
- [17] Dixit A, Gade U. A case study on human bio-heat transfer and thermal comfort within CFD. *Building Environment*. 2015;94:122-30.
- [18] Khatoon S, Kim M-H. Human thermal comfort and heat removal efficiency for ventilation variants in passenger cars. *Energies*. 2017;10(11):1710.
- [19] Curre J, Maué J. Numerical study of the influence of air vent area and air mass flux on the thermal comfort of car occupants. *SAE Technical Paper*; 2000. Report No.: 0148-7191.
- [20] Alahmer A, Mayyas A, Mayyas AA, Omar M, Shan D. Vehicular thermal comfort models; a comprehensive review. *Applied Thermal Engineering*. 2011;31(6-7):995-1002.
- [21] Li J, Cao X, Liu J, Mohanarangam K, Yang W. PIV measurement of human thermal convection flow in a simplified vehicle cabin. *Building Environment*. 2018;144:305-15.
- [22] Hubakri MF, Zamri MAS, Hamzah MNA, Roslan RA, Wan Ab Naim WN, Mohamed Mokhtarudin MJ. Design and development of a flexible test rig for biomedical engineering PIV experiment. *Enabling Industry 40 through Advances in Manufacturing and Materials: Selected Articles from iM3F 2021, Malaysia: Springer; 2022. p. 99-107.*